Supramolecular Chemistry
Publication details, including instructions for authors and subscription information:
http://www.informaworld.com/smpp/title~content=t713649759

Polymer deaggregation and assembly controlled by a double cavity cucurbituril

Regan Nally[a]; Oren A. Scherman[b]; Lyle Isaacs[a]
[a] Department of Chemistry and Biochemistry, University of Maryland, College Park, MD, USA [b] Melville Laboratory for Polymer Synthesis, Department of Chemistry, University of Cambridge, Cambridge, CB2 1EW, UK

To cite this Article Nally, Regan , Scherman, Oren A. and Isaacs, Lyle(2010) 'Polymer deaggregation and assembly controlled by a double cavity cucurbituril', Supramolecular Chemistry, 22: 11, 683 — 690, First published on: 18 November 2010 (iFirst)

To link to this Article: DOI: 10.1080/10610278.2010.497213

URL: http://dx.doi.org/10.1080/10610278.2010.497213

Supramolecular Chemistry
Vol. 22, Nos. 11–12, November–December 2010, 683–690

Polymer deaggregation and assembly controlled by a double cavity cucurbituril[†]

Regan Nally[a], Oren A. Scherman[b]* and Lyle Isaacs[a]*

[a]*Department of Chemistry and Biochemistry, University of Maryland, College Park, MD 20742, USA;* [b]*Melville Laboratory for Polymer Synthesis, Department of Chemistry, University of Cambridge, Lensfield Road, Cambridge CB2 1EW, UK*

(*Received 6 April 2010; final version received 26 May 2010*)

A supramolecular polymer was prepared from a mixture of poly(diallyldimethylammonium chloride) (**1**) and bis-*ns*-CB[10]. The repeat units of the polymer chain are capable of binding inside each of the two cavity domains of bis-*ns*-CB[10]. The bis-*ns*-CB[10] molecular containers complex the sides of the polymer chain – which we term a cupping interaction – thereby promoting the association of individual polymer strands to form $\mathbf{1}_n$·bis-*ns*-CB[10]$_m$, which results in an extension of the length of the polymer. The effect of bis-*ns*-CB[10] on the physical properties of the polymer was investigated using viscometry in dilute aqueous solution. A decrease in η_{rel} was observed upon increasing the concentrations of bis-*ns*-CB[10] to a solution of **1**. Atomic force microscopy and diffusion-ordered spectroscopy were performed to probe the mode of interaction between polymer **1** and bis-*ns*-CB[10]. Collectively, the data support the two roles for bis-*ns*-CB[10]: (1) as a deaggregation agent at lower concentrations and (2) as a cupping agent that non-covalently links individual polymer strands at higher concentrations resulting in overall extension of the polymer.

Keywords: supramolecular polymer; cucurbituril; viscometry

1. Introduction

Polymers give rise to a diversity of materials enabling constant improvement to our daily lives: from beverage containers, automotive parts and textiles, to prosthetics and extreme weather materials (*1*). Although the contributions made by covalent polymers to the development of industries are substantial, there are always improvements to be made. An ongoing challenge in the realm of polymer chemistry is the ability to control the properties of polymers through incremental changes in their structures or to alter external variables (pH, temperature, concentration, etc.). An alternative approach to controlling polymer properties involves their assembly by non-covalent interactions rather than by covalent bonds. Such supramolecular polymers (*2*) may assume a variety of geometries by the assembly of monomeric units through non-covalent interactions in *n*-dimensional patterns (linear, branched, dendritic, etc.). Most significant, however, is the high stimuli responsiveness of supramolecular polymers, which make them ideal systems to control polymer properties in a straightforward manner.

The existence of supramolecular polymers is widespread, from their biological function as microtubules, microfilaments, viruses, phages and proteins, to their synthetic production as potential coatings, inks and adhesives. The sensitivity of these systems to changes in pH, temperature, concentration and solvent translates to changes in the properties of the bulk material. For example, the sensitivity towards mechanical stress can be capitalised upon with a self-healing rubber composed of molecules containing amido functionality for hydrogen bonding. This material can undergo multiple cycles of stretching, breaking and mending (*3a*). These mechanical properties may be useful in coatings, where the material once applied to a surface can be heat treated to repair the coating rather than adding another layer of material.

Solution viscosity is a particularly important property of a material and the ability to control viscosity poses a challenge to chemists. Supramolecular polymers typically possess low-viscosity melts, wherein a small increase in temperature leads to a large decrease in viscosity due to the breaking of weak intermolecular interactions. This decrease in viscosity results in more straightforward processability, such as creation of a surface coating. Covalent polymers, in contrast, require high temperature and pressure to achieve a decrease in viscosity (*3b*). The ability to modify the viscosity of a solution by temperature, concentration or chemical stimulus is valuable to the materials as well as to food industries. For example, the mouth-feel of coffee is enhanced by optimising the viscosity to a certain range by the addition of arabinogalactans (*4*). Accordingly, the tunable

---

*Corresponding authors. Emails: oas23@cam.ac.uk; lisaacs@umd.edu
[†]Dedicated to the memory of Prof. Dmitry Rudkevich

ISSN 1061-0278 print/ISSN 1029-0478 online

DOI: 10.1080/10610278.2010.497213
http://www.informaworld.com

properties of non-covalent materials render them prime systems for a wide array of applications.

The properties of supramolecular polymers stem from the structures of their monomeric units. For example, non-covalent association of monomers based on metal–ligand coordination (*5–7*), hydrogen bonding (*8–12*), aromatic stacking (*13*, *14*) and host–guest interactions (*15–18*) has resulted in formation of supramolecular polymeric systems. Of particular note are the self-complementary ureidopyrimidinone dimers of the A—A type reported by Meijer, Sijbesma and co-workers (*12*), which undergo assembly through quadruple hydrogen-bonding interactions to form a homomeric supramolecular polymer. The success of this system is in large part due to the high affinity ($\approx 10^{7}\,\mathrm{M}^{-1}$) with which the monomers dimerise, resulting in a high degree of polymerisation. Host–guest chemistry has also been shown to generate supramolecular polymers. For example, Harada has incorporated a guest-derivatised cyclodextrin as an A—B monomeric unit to achieve construction of main chain and branched polymers of the $(\cdots\mathrm{A{-}B}\cdots\mathrm{A{-}B}\cdots)_n$ type (*16*, *17*, *19*). One limitation of this cyclodextrin–guest system is the modest affinities ($K_\mathrm{a} \approx 10^{4}\,\mathrm{M}^{-1}$) of these types of A···B interactions which limit the overall degree of polymerisation.

The cucurbit[*n*]uril (CB[*n*]) family of macrocycles is known for its high binding affinities (K_a up to 10^{15}) (*20–22*) and selectivities (K_rel up to 10^{7}) (*23*) towards aliphatic and aromatic amines. Guests bind to CB[*n*] through the hydrophobic effect to the interior of the CB cavity and through cation–dipole interactions between the carbonyl-lined portals of the CB[*n*] and ammonium functionality of the guest. The range of different cavity volumes for CB[5]–CB[8] and CB[10] (82–870 Å^3) allows for the recognition of a wide variety of guests. These recognition abilities allow CB[*n*] to be tailored to a range of applications, including waste-stream remediation (*24*, *25*), chemical sensing (*26*, *27*), molecular machines (*28–30*) and supramolecular materials (*31–33*). Of direct relevance to the work reported herein are reports from the Kim and Scherman groups regarding the preparation of supramolecular polymers using the ability of CB[8] to promote 1:1:1 ternary complexes. For example, the Scherman group has successfully prepared a supramolecular block copolymer from polymers end functionalised with viologen and naphthalene units (*18*). Kim has combined CB[8] with divalent and trivalent building blocks in the construction of higher order supramolecular oligomeric and dendritic complexes (*34*, *35*).

Over the past several years, our group has been interested in the supramolecular chemistry of *nor-seco*-CB[*n*], which by virtue of their new structurally responsive architectures display interesting behaviour. For example, (±)-bis-*ns*-CB[6] and bis-*ns*-CB[10] have displayed chiral recognition properties and homotropic allosteric behaviour, respectively (*36*, *37*). The high selectivity and affinity of CB[*n*] towards ammonium ion guests encouraged us to work on the formation of discrete and polymeric complexes comprising bis-*ns*-CB[10] (Figure 1). Of the *ns*-CB[*n*] isolated thus far, bis-*ns*-CB[10] is unique in that it possesses two identical cavities. Accordingly, bis-*ns*-CB[10] is a prime host for the generation of an $(\mathrm{A{-}A}\cdots\mathrm{B{-}B}\cdots)_n$ type supramolecular polymer (Figure 2(c)).

2. Results and discussion

First, we briefly present our previous results that led to the experiments performed herein as well as the design strategy of our present findings. Then, we discuss the experimental data that formulated our final interpretation of this system. And lastly, we close with an explanation of our work and potential applications of this research.

3. Design strategy

Previously, we reported studies directed towards the generation of a supramolecular polymer from bis-*ns*-CB[10] and guests **2** and **3**. Experimentally, we found that divalent guest molecules are capable of forming 1:1 (Figure 2(a)) or 2:2 (Figure 2(b)) complexes with bis-*ns*-CB[10], where the length of the rigid linker between the two adamantyl groups dictates the molecularity of the resulting complex. We believe that a supramolecular polymer did not form due to (1) the low solubility of bis-*ns*-CB[10], which limited the concentrations to the micro molar range, (2) the absence of a bulky group on the linker to prevent two guests from side-by-side orientation, as shown in the 2:2 complex (Figure 2(b)) or (3) the short length of the linker, which preorganised the complex to form a closed (1:1) system (*38*). We, therefore, turned our attention to linker length, and hypothesised that if we used a polymeric guest capable of binding inside the cavity of bis-*ns*-CB[10], we could generate a supramolecular polymer, as its extended length would deter formation of discrete complexes (Figure 2(a) and (b)). For this purpose,

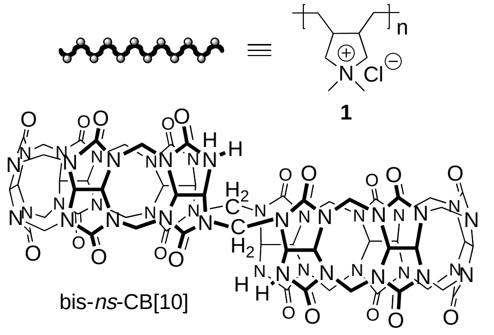

Figure 1. Schematic depiction of polymer (**1**) and the chemical structure of host bis-*ns*-CB[10].

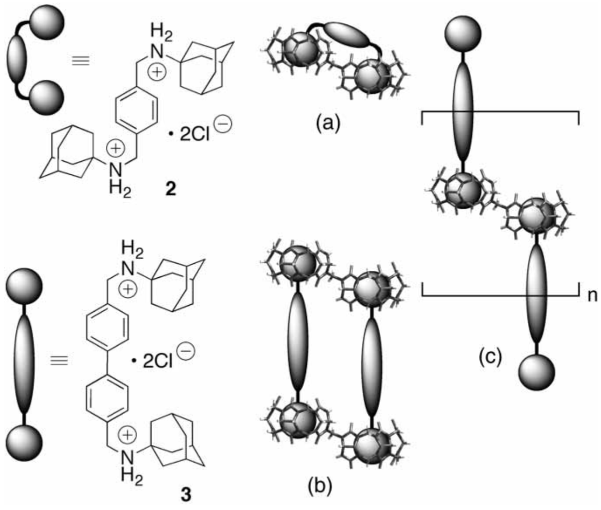

Figure 2. Schematic representation of adamantanediammonium guests **2** and **3** with corresponding host–guest inclusion complexes: (a) bis-*ns*-CB[10]·**2**, (b) bis-*ns*-CB[10]$_2$·**3**$_2$ and (c) hypothetical linear polymer comprising bis-*ns*-CB[10] and **3**.

we chose poly(diallyldimethylammonium) chloride, **1**, with a molecular weight range of 100,000–200,000 g/mol. Polymer **1** is a polyelectrolyte that assumes a rod-like conformation in dilute aqueous solution and is capable of aggregating through counterion-induced attractions (*39–42*). According to computer modelling (Spartan), the length of **1** spans the range of 270–540 nm. This polyelectrolyte has been implemented as a displacer for cation-exchange displacement chromatography of proteins (*43*) and as a substrate for ultra-thin polyelectrolyte multilayer films (*40*, *44*). This polymeric polycation (**1**) exhibits excellent solubility in water and its ammonium-tagged repeat units have the potential to bind within the cavities of bis-*ns*-CB[10].

A priori, the interaction between bis-*ns*-CB[10] and **1** could proceed by several different geometrical modes of interaction. Figure 3 represents several of the most plausible modes of interaction. To begin, the degree to which **1** (Figure 3(a)) self-associates (e.g. $(\mathbf{1})_n$ where n refers to the number of aggregating polymer chains, not the number of monomeric units in each polymer chain, Figure 3(b)) is concentration dependent, as the non-covalent interactions are reversible. The introduction of bis-*ns*-CB[10] to a solution of **1** can generate the formation of a new assembly. For example, bis-*ns*-CB[10] could bind to the terminal unit of **1** and stay put or thread along the main chain. We do not believe that bis-*ns*-CB[10] threads onto **1**, because addition of a competitive guest (*vide infra*) results in rapid complexation with bis-*ns*-CB[10]. The threading process could potentially be driven by addition of excess bis-*ns*-CB[10] to a solution of **1**, creating **1**·bis-*ns*-CB$[10]_n$ species. One such result of threading behaviour is the construction of a ladder assembly (Figure 3(c)) or the kinking of polymer **1** (Figure 3(d)), similar to a β-hairpin turn in polypeptide folding. The entropic penalty for the formation of both these structures would require high enthalpic gains. Conversely, if bis-*ns*-CB[10] binds to the outside of **1**, it could act as an agent that promotes the deaggregation of $(\mathbf{1})_n$, which could further act as a supramolecular polymerising agent, linking individual polymer strands together (Figure 3(e)). The picture could grow increasingly complex, as we consider the concentration, stoichiometries and dynamic equilibrium of the system. To understand the influence of bis-*ns*-CB[10] on an aqueous solution of **1**, we performed viscosity measurements, atomic force miscroscopy (AFM) imaging and diffusion-ordered NMR spectroscopy (DOSY) experiments.

3.1 *Viscosity measurements*

We anticipated that the addition of bis-*ns*-CB[10] to a solution of **1** would cause an increase in the solution viscosity, functioning to non-covalently link polymer

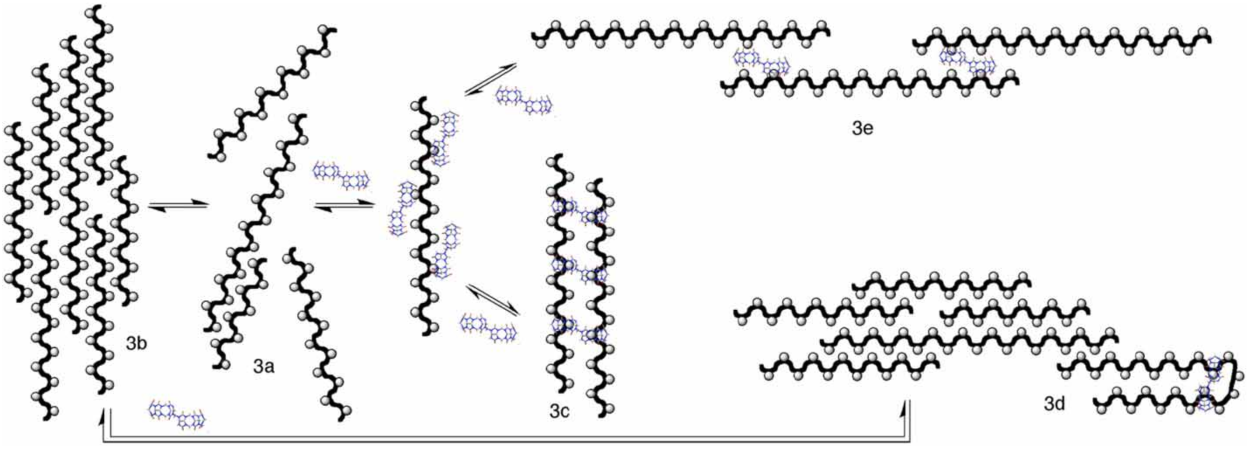

Figure 3. Depiction of the potential equilibria between various possible forms of mixtures of **1** and bis-*ns*-CB[10].

strands together, and thus lengthening the polymer (e.g. Figure 3(a)–(e)). We investigated the viscosity of a solution of **1** upon addition of bis-*ns*-CB[10] or CB[7] to ascertain whether a double-cavity CB would behave differently from its single-cavity relatives (CB[5]–CB[8]) and translate to a difference in solution properties. This hypothetical increase in viscosity should be unique to a solution containing **1** and bis-*ns*-CB[10] when compared with a solution containing **1** and CB[7], as each of its two cavities of bis-*ns*-CB[10] can encapsulate a terminal pyrrolidine unit of **1**.

Mixtures of **1** with CB[6], CB[7], CB[8] or bis-*ns*-CB[10] in water were heated at 50°C for 8 h. At this time, CB[6] and CB[8] remained insoluble, even at concentrations below 100 μM, confirming the absence of non-covalent interactions between **1** and CB[6], and between **1** and CB[8]. Upon reaching room temperature, homogeneous solutions containing CB[7] (46–460 μM) and **1** (333 μM) or bis-*ns*-CB[10] (46–368 μM) and **1** (333 μM) were filtered, and viscosity measurements were performed at 25°C. Figure 4 shows a plot of η_{rel} vs. the concentration of CB. Solutions containing **1** and CB[7] did not exhibit significant changes in viscosity relative to a solution containing **1** alone. The addition of bis-*ns*-CB[10] to a solution of **1**, however, caused a decrease in the relative viscosity. This trend continued with addition of bis-*ns*-CB[10], until the concentration reached 368 μM, at which point, the solution became heterogeneous. This result was puzzling as it conflicted with our hypothesis that addition of bis-*ns*-CB[10] to a solution of **1** should increase the hydrodynamic radius of the polymer through host–guest interactions, which should in turn translate to an increase in viscosity. To try to understand this unexpected result, we decided to use other techniques to gain insight into the mode of interaction between **1** and bis-*ns*-CB[10].

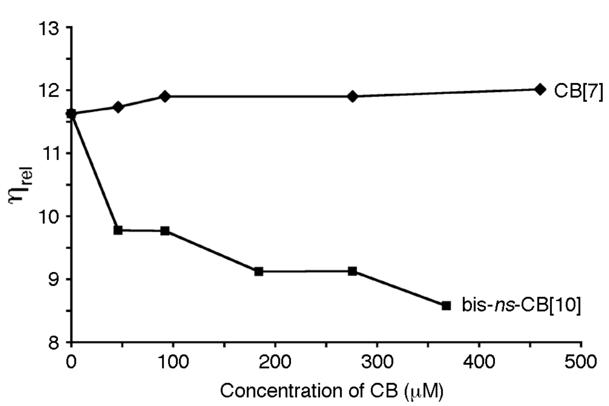

Figure 4. Plot of relative viscosity of **1** (polymer concentration = 333 μM) vs. concentration of CB. Legend: ■ = bis-*ns*-CB[10], ◆ = CB[7].

3.2 ^{1}H NMR

^{1}H NMR can provide information regarding the geometry and strength of host–guest binding interactions. To provide evidence for the inclusion of a pyrrolidinium unit within the cavity of bis-*ns*-CB[10], ^{1}H NMR spectra were recorded for solutions containing **1** alone and with bis-*ns*-CB[10] (Figure 5). The ^{1}H NMR spectrum of a solution of **1** (Figure 5(a)) does not display resonances below 1 ppm. Figure 5(b) shows the spectrum recorded for a solution containing **1** and bis-*ns*-CB[10], displaying upfield shifted polymer peaks, representing an inclusion of the polypyrrolidinium unit within the cavity of bis-*ns*-CB[10]. The ratio of bis-*ns*-CB[10] to **1** is 0.08. Therefore, the peaks representing **1** bound inside bis-*ns*-CB[10] are less intense when compared with those of the unbound polymer. If we add a competitive guest to a solution containing **1** and bis-*ns*-CB[10], we could potentially observe disappearance of the resonances for bound **1**, and appearance of resonances for the bound competing guest. This would tell us if the resonances below 1 ppm in

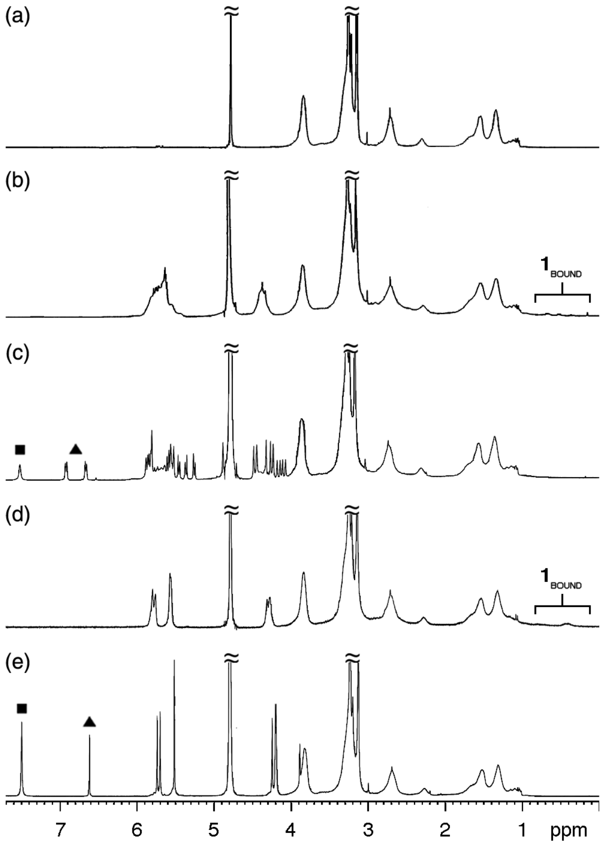

Figure 5. ^{1}H NMR spectra (400 MHz, D_2O, RT) recorded for solutions of (a) **1** (polymer concentration = 30 μM), (b) **1** (polymer concentration = 232 μM) and bis-*ns*-CB[10] (232 μM), (c) **1** (polymer concentration = 232 μM), bis-*ns*-CB[10] (232 μM) and **4** (464 μM), (d) **1** (polymer concentration = 232 μM) and CB[7] (232 μM) and (e) **1** (polymer concentration = 232 μM), CB[7] and **4**. ■, free **4**; ▲, bound **4**.

Figure 5(b) are due to reversible, non-covalent interactions between **1** and bis-*ns*-CB[10], and that the competing guest has a higher affinity for bis-*ns*-CB[10] than monomeric units of **1**. For this purpose, we chose *p*-xylylenediamine, **4** (Chart 1), as a competitive guest whose affinity for various CB[*n*] has been well documented (*21*). Upon addition of **4** to a solution containing **1** and bis-*ns*-CB[10], the presence of bound polymer peaks disappear (within 6 min), and we observe resonances for both free and bound **4**. Compound **4** is a competing guest to polymer **1** and bis-*ns*-CB[10] prefers inclusion of **4** over **1**. An analogous experiment was carried out with CB[7], whereby **4** was added to a solution containing **1** and CB[7]. Figure 5(d) shows the ^{1}H NMR spectra recorded for a solution containing **1** and CB[7]. Resonances below 1 ppm are observed and we attribute this to bound pyrrolidinium units within CB[7]. Figure 5(e) shows the ^{1}H NMR spectrum recorded for a solution containing **1**, CB[7] and **4**. Again, the peaks corresponding to bound polymer, **1**, disappear and the presence of bound **4** within CB[7] is apparent. The results of the ^{1}H NMR experiments show that both bis-*ns*-CB[10] and CB[7] have a greater affinity for **4** than for **1**. The response of the system to an external stimulus illustrates its dynamic behaviour and offers indirect proof that the ^{1}H NMR peaks appearing below 1 ppm arise due to pyrrolidinium units of **1** being bound to bis-*ns*-CB[10] or CB[7]. Having confirmed the binding of **1** within the cavity of bis-*ns*-CB[10], we wanted to understand how this interaction was able to cause a decrease in solution viscosity. We considered that bis-*ns*-CB[10] could be inducing a conformational change within the polymer chains, from linear to kinked (Figure 3(d)), which may alter the degree to which it self-associates. Evidence of conformational change could provide insight into the mechanism of binding and offer a plausible reason for the observed viscosity trend.

3.3 Atomic force microscopy

With the challenges inherent in characterising the supramolecular systems, imaging offers the most direct evidence – albeit with the usual caveats regarding the potential for structural differences between the solution and surface – for changes in the topology of a macromolecular assembly. To gain information about the shape of polymer **1** alone and in the presence of bis-*ns*-CB[10], we performed AFM imaging (Figure 6). To ensure that the images generated were representative of the sample as a whole, each sample was imaged in at least five different locations.

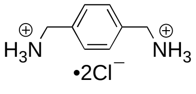

4

Chart 1. Chemical structure of *p*-xylylenediamine dihydrochloride (**4**).

Spin-casting solutions of **1** (7 μM in H_2O) onto freshly cleaved mica delivered the amplitude images shown in Figure 6(a) and (b). Figure 6(c) and (d) are amplitude images of a dried solution containing **1** (7 μM) and bis-*ns*-CB[10] (7 μM). The most obvious difference between solutions of **1** and **1** with bis-*ns*-CB[10] is the presence of extended linear structures in Figure 6(c). We believe this reflects the formation of a supramolecular polymer constructed from bis-*ns*-CB[10] linking several individual strands of **1**. To estimate the size difference between the polymers shown in Figure 6(a) and (c), the lengths of 10 structures from each image were measured. The average structure length recorded from Figure 6(a) was 184 nm and that from Figure 6(c) was 1000 nm. Upon further analysis of the images, we noticed that the structure in Figure 6(b) also appears wider than that in Figure 6(d). We surmised that deaggregation of clusters of **1** may translate to an overall decrease in solution viscosity. To ascertain the possibility of bis-*ns*-CB[10] causing deaggregation of clusters of **1**, we conducted a bearing analysis. Bearing analysis is a method of analysing the distribution of surface height over a sample (*45*). The collection of feature heights based upon the occurrence of data points at various *z* heights is presented as a histogram. Height images were captured and bearing analyses performed on the longest structures from both the images of **1** alone and from **1** and

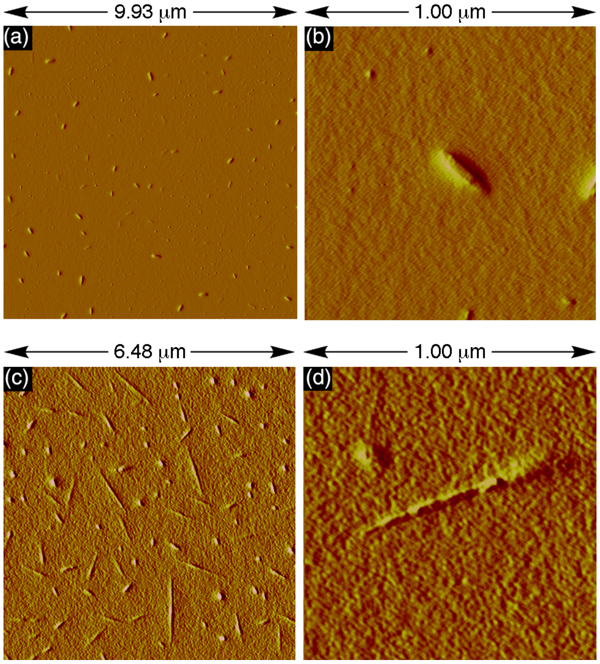

Figure 6. AFM amplitude images of **1** (polymer concentration = 7 μM) from (a) 9.93 μm scan area and (b) 1.00 μm scan area, and **1** (polymer concentration = 7 μM) with bis-*ns*-CB[10] (7 μM) from (c) 6.48 μm scan area and (d) 1.00 μm scan area.

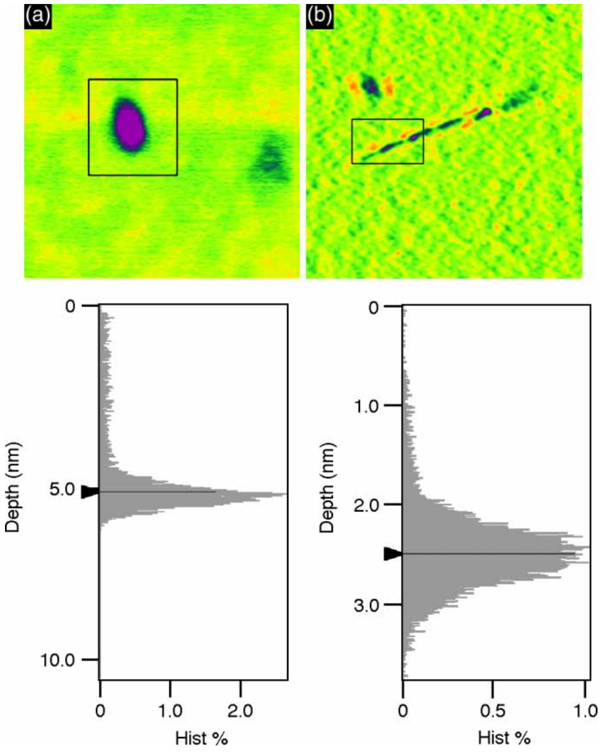

Figure 7. AFM height images and corresponding bearing analysis histograms for a sample containing (a) **1** alone and (b) **1** with bis-*ns*-CB[10]. Boxed region within the images is the area used for sampling to generate histogram (directly below).

bis-*ns*-CB[10]. The average heights differed from 6.8 nm from an image of **1** alone to 2.3 nm from an image of **1** and bis-*ns*-CB[10].

Figure 7 shows the representative bearing analyses where the average depth of a structure from the sample containing only **1** is 5.2 nm and that from the sample containing **1** and bis-*ns*-CB[10] is 2.5 nm. These measurements provide evidence for the role of bis-*ns*-CB[10] as a deaggregation agent of clusters of polymer strands (e.g. Figure 3(b)–(e)). To provide evidence for the increase in the size of the polymer assembly, we employed diffusion-ordered NMR spectroscopy.

3.4 Diffusion NMR

DOSY measures the rate of diffusion of a molecule through solution. In line with our thinking of the role of bis-*ns*-CB[10] as a cupping agent that induces elongation (Figure 3(e)), the diffusion rate of the polymer should decrease as it is lengthened. If bis-*ns*-CB[10] instead threaded on to **1** (Figure 3(c) or (d)), the complex would diffuse through solution at approximately the same rate as **1** alone. Alternatively, as we observed a decrease in the viscosity of a solution containing **1** upon addition of bis-*ns*-CB[10], we could also rationalise an increase in the diffusion rates obtained from a solution of **1** and bis-*ns*-CB[10] when compared with a solution of **1** alone

$$D_{\mathrm{s}} = \frac{k_{\mathrm{B}}T}{6\check{s}\eta R}. \qquad (1)$$

According to the Stokes–Einstein Equation (1), the diffusion coefficient of a sphere (D_{s}) is inversely related to the hydrodynamic radius (R) and solvent viscosity (η), where k_{B} is Boltzmann's constant and T is the temperature. As our polymer, **1**, is cylindrical, we resort to evaluating the measurements qualitatively. The diffusion coefficient obtained from a 33-μM solution of **1** alone is $D_{\mathrm{s}} = 1.2 \times 10^{-10}\,\mathrm{m^2/s}$ and the value from a solution of **1** (33 μM) and bis-*ns*-CB[10] (260 μM) is $D_{\mathrm{s}} = 6.8 \times 10^{-11}\,\mathrm{m^2/s}$. The theory of diffusion NMR measurements predicts that the value of the $D_{n\text{-mer}}/D_{\mathrm{monomer}}$ ratio reflects a change in the size of the assembly (*46*). For example, a $D_{n\text{-mer}}/D_{\mathrm{monomer}} = 0.79$ corresponds to a dimeric assembly. By substitution of the D_{s} value for the *n*-mer (**1** and bis-*ns*-CB[10]) over the D_{s} value for the *monomer* (**1**), we obtain a value of 0.57. Theory predicts a $D_{n\text{-mer}}/D_{\mathrm{monomer}}$ value of 0.59 for a pentameric species and 0.55 for a hexameric species. Though we cannot draw absolute conclusions from this numerical comparison, the $D_{n\text{-mer}}/D_{\mathrm{monomer}}$ ratio is an indication of the formation of an assembled oligomeric species comprising **1** and bis-*ns*-CB[10] in solution. From the viscosity data (Figure 4), it is seen that a solution containing **1** and bis-*ns*-CB[10] is less viscous than a solution containing **1** alone. The Stokes–Einstein equation shows that viscosity is inversely proportional to the rate of diffusion. Accordingly, we would expect to observe a faster rate of diffusion for a solution containing **1** and bis-*ns*-CB[10] than for **1** alone. Yet, we observed the opposite trend experimentally. The hydrodynamic radius (R) is the remaining variable in the Stokes–Einstein equation that affects the rate of diffusion. Therefore, our unexpected observation of a slower diffusion rate of **1** in the presence of bis-*ns*-CB[10] relative to **1** alone must reflect a much larger hydrodynamic radius of the polymeric species in a solution containing **1** and bis-*ns*-CB[10] relative to **1** alone. The most plausible explanation, guided by the evidence provided herein, is that the viscosity is decreased as a result of bis-*ns*-CB[10] deaggregating clusters of **1** and concomitantly inducing non-covalent polymerisation. These DOSY results support the AFM images, accounting for the increase in hydrodynamic radius leading to slower diffusion rates of the extended polymer.

4. Conclusion

In summary, we have shown that bis-*ns*-CB[10] is able to link separate strands of **1** together, generating a supramolecular polymer (Figure 3(e)) in solution, which remains intact in the bulk. The observed decrease in viscosity of a solution of **1** upon addition of bis-*ns*-CB[10] is best explained with AFM images, where bis-*ns*-CB[10] (1) induces deaggregation of **1** and (2) extends the length of the polymer. This is supported by an increase in hydrodynamic radius as evidenced by DOSY NMR spectroscopy. Therefore, the decrease in chain–chain interactions (entanglement) for **1** is more pronounced at higher concentrations (330 μM), whereby introduction of bis-*ns*-CB[10] leads to deaggregation; on the other hand, introduction of bis-*ns*-CB[10] to a more dilute solution of **1** (33 μM) leads to an elongation of the polymer chains.

The formation of a new material opens doors for further properties analysis. This supramolecular polymer may display temperature-dependent properties that could be used, for example, in the preparation of hot melts (applications towards the manufacturing of books, shoes, cartons, envelopes, labels, aircraft, etc.). As shown in this paper, bis-*ns*-CB[10] is a powerful viscosity modulator, and therefore, may affect the solution viscosity of other systems as well. Owing to the reversible nature of the $\mathbf{1}_n$·bis-*ns*-CB$[10]_m$ assembly, the system can be tested for its reaction to external stimuli. The potential sensitivity of this material towards external stimuli may find applications in supramolecular photonics and electronics.

5. Experimental details

Starting materials were purchased from commercial suppliers and used without further purification. Poly (diallyldimethylammonium chloride), **1**, was purchased from Sigma-Aldrich (St Louis, MO, USA) and used without further purification. Polymer **1** has an average molecular weight range of 100,000–200,000 g/mol. Bis-*ns*-CB[10] was prepared according to the literature procedure (*36*). All solutions of **1** were allowed to warm at 50°C for 8 h, and then cooled to room temperature and filtered through a PTFE filter (0.2 μm) prior to analysis. Solution viscosities were measured using a Schott–Geräte Ubbelohde microviscometer with a suspended level bulb using a processor viscosity system 1 (PVS1) measuring device. The microviscometer was thermostated in a PV15 water bath at 25.00 (± 0.01)°C using a DLK10 thermostat unit (Lauda). NMR experiments were performed on Bruker AV400 and AVIII600 instruments operating at 400 and 600 MHz, respectively. Chemical shifts were referenced to the solvent values (δ 4.79 ppm for HOD). ^{1}H NMR spectra were recorded at 25°C (calibration with MeOH) and DOSY experiments were recorded at 40°C (calibration with ethylene glycol). AFM samples were prepared by spin-casting solutions onto a freshly cleaved mica surface. Sample imaging was carried out in air at ambient temperature on an apparatus by Digital Instruments, Inc. (Tonawanda, NY, USA) in tapping mode. The cantilever-tip systems used were manufactured by Veeco from antimony-doped silicon, having an 8-nm tip radius. The height and amplitude images and bearing analysis were performed with NanoScope III software.

Acknowledgements

We would like to thank the members of the Scherman group for instructive conversations. We thank the National Science Foundation (CHE-0615049 and CHE-0829337 to LI), the Department of Education (P200A060238-07, GAANN fellowship to RN) and the UK Engineering and Physical Sciences Research Council (EP/F035535) and the Walters–Kundert Trust (OAS) for financial support.

References

(1) Stevens, M.P. *Polymer Chemistry*, 3rd ed.; Oxford University Press: New York, 1999.
(2) For reviews of supramolecular polymers see: Moore, J.S. *Curr. Opin. Colloid Interface Sci.* **1999,** *4*, 108–116; Corbin, P.S.; Zimmerman, S.C. *Supramol. Polym.* **2000,** 147–176; Brunsveld, L.; Folmer, B.J.B.; Meijer, E.W.; Sijbesma, R.P. *Chem. Rev.* **2001,** *101*, 4071–4097; Weck, M. *Polym. Int.* **2007,** *56*, 453–460; Fox, J.D.; Rowan, S.J. *Macromolecules* **2009,** *42*, 6823–6835; Harada, A.; Takashima, Y.; Yamaguchi, H. *Chem. Soc. Rev.* **2009,** *38*, 875–882.
(3) (a) Cordier, P.; Tournilhac, F.; Soulié-Ziakovic, C.; Leibler, L. *Nature* **2008,** *451*, 977–980. (b) de Greef, T.F.A.; Meijer, E.W. *Nature* **2008,** *453*, 171–173.
(4) Curti, D.G.; Gretsch, C.; Labbe, D.P.; Redgwell, R.J.; Schoonman, J.H.; Ubbink, J.B. *Arabinogalactan Isolate from Coffee*. PCT/EP2005/004084, 2005.
(5) Michelsen, U.; Hunter, C.A. *Angew. Chem., Int. Ed.* **2000**, *39*, 764–767.
(6) Velten, U.; Rehahn, M.G.S. *Chem. Commun.* **1996**, 2639–2640.
(7) Hofmeier, H.; Hoogenboom, R.; Wouters, M.E.; Schubert, U.S. *J. Am. Chem. Soc.* **2005**, *127*, 2913–2921.
(8) Simic, V.; Bouteiller, L.; Jalabert, M. *J. Am. Chem. Soc.* **2003**, *125*, 13148–13154.
(9) Beck, J.B.; Rowan, S.J. *J. Am. Chem. Soc.* **2003**, *125*, 13922–13923.
(10) Bladon, P.; Griffin, A.C. *Macromolecules* **1993**, *26*, 6604–6610.
(11) Gulik-Krzywicki, T.; Fouquey, C.; Lehn, J.-M. *Proc. Natl Acad. Sci. USA* **1993**, *90*, 163–167.
(12) Sijbesma, R.P.; Beijer, F.H.; Brunsveld, L.; Folmer, B.J.; Hirschberg, J.H.; Lange, R.F.; Lowe, J.K.; Meijer, E.W. *Science* **1997**, *278*, 1601–1604.
(13) Gabriel, G.J.; Sorey, S.; Iverson, B.L. *J. Am. Chem. Soc.* **2005**, *127*, 2637–2640.
(14) Markovitsi, D.; Bengs, H.; Ringsdorf, H. *J. Chem. Soc., Faraday Trans.* **1992**, *88*, 1275–1279.
(15) Li, G.; McGown, L.B. *Science* **1994**, *264*, 249–251.
(16) Miyauchi, M.; Harada, A. *J. Am. Chem. Soc.* **2004**, *126*, 11418–11419.
(17) Miyawaki, A.; Takashima, Y.; Yamaguchi, H.; Harada, A. *Tetrahedron* **2008**, *64*, 8355–8361.
(18) Rauwald, U.; Scherman, O.A. *Angew. Chem., Int. Ed.* **2008**, *47*, 3950–3953.
(19) Hasegawa, Y.; Miyauchi, M.; Takashima, Y.; Yamaguchi, H.; Harada, A. *Macromolecules* **2005**, *38*, 3724–3730.

(20) Rekharsky, M.V.; Mori, T.; Yang, C.; Ko, Y.H.; Selvapalam, N.; Kim, H.; Sobransingh, D.; Kaifer, A.E.; Liu, S.; Isaacs, L.; Chen, W.; Moghaddam, S.; Gilson, M.K.; Kim, K.; Inoue, Y. *Proc. Natl Acad. Sci. USA* **2007**, *104*, 20737–20742.

(21) Liu, S.; Ruspic, C.; Mukhopadhyay, P.; Chakrabarti, S.; Zavalij, P.Y.; Isaacs, L. *J. Am. Chem. Soc.* **2005**, *127*, 15959–15967.

(22) Jeon, W.S.; Moon, K.; Park, S.H.; Chun, H.; Ko, Y.H.; Lee, J.Y.; Lee, E.S.; Samal, S.; Selvapalam, N.; Rekharsky, M.V.; Sindelar, V.; Sobransingh, D.; Inoue, Y.; Kaifer, A.E.; Kim, K. *J. Am. Chem. Soc.* **2005**, *127*, 12984–12989.

(23) Isaacs, L. *Chem. Commun.* **2009**, 619–629.

(24) Dantz, D.A.; Meschke, C.; Buschmann, H.-J.; Schollmeyer, E. *Supramol. Chem.* **1998**, *9*, 79–83.

(25) Kornmuller, A.; Karcher, S.; Jekel, M. *Water Res.* **2001**, *35*, 3317–3324.

(26) Praetorius, A.; Bailey, D.M.; Schwarzlose, T.; Nau, W.M. *Org. Lett.* **2008**, *10*, 4089–4092.

(27) Reczek, J.J.; Kennedy, A.A.; Halbert, B.T.; Urbach, A.R. *J. Am. Chem. Soc.* **2009**, *131*, 2408–2415.

(28) Lee, J.J.C.; Kim, K.; Kim, K. *Chem. Commun.* **2001**, 1042–1043.

(29) Ong, W.; Gómez-Kaifer, M.; Kaifer, A.E. *Org. Lett.* **2002**, *4*, 1791–1794.

(30) Ko, Y.H.; Kim, E.; Hwang, I.; Kim, K. *Chem. Commun.* **2007**, 1305–1315.

(31) Kim, K.; Jeon, W.S.; Kang, J.K.; Lee, J.W.; Jon, S.Y.; Kim, T.; Kim, K. *Angew. Chem., Int. Ed.* **2003**, *42*, 2293–2296.

(32) Kim, K.; Kim, D.; Lee, J.W.; Ko, Y.H.; Kim, K. *Chem. Commun.* **2004**, 848–849.

(33) Sokolov, M.; Virovets, A.; Dybtsev, D.; Gerasko, O.; Fedin, V.; Hernandez-Molina, R.; Clegg, W.; Sykes, A. *Angew. Chem., Int. Ed.* **2000**, *39*, 1659–1661.

(34) Ko, Y.H.; Kim, K.; Kang, J.K.; Chun, H.; Lee, J.W.; Sakamoto, S.; Yamaguchi, K.; Fettinger, J.C.; Kim, K. *J. Am. Chem. Soc.* **2004**, *126*, 1932–1933.

(35) Kim, S.-Y.; Ko, Y.H.; Lee, J.W.; Sakamoto, S.; Yamaguchi, K.; Kim, K. *Chem. Asian J.* **2007**, *2*, 747–754.

(36) Huang, W.H.; Liu, S.; Zavalij, P.Y.; Isaacs, L. *J. Am. Chem. Soc.* **2006**, *128*, 14744–14745.

(37) Huang, W.-H.; Zavalij, P.Y.; Isaacs, L. *Angew. Chem., Int. Ed.* **2007**, *46*, 7425–7427.

(38) Chen, C.; Dormidontova, E. *Macromolecules* **2004**, *37*, 3905–3917.

(39) Mirenda, M.; Dicelio, L.E.; San Román, E. *J. Phys.: Condens. Matter* **2008**, *112*, 12201–12207.

(40) McAloney, R.A.; Sinyor, M.; Dudnik, V.; Goh, M.C. *Langmuir* **2001**, *17*, 6655–6663.

(41) Guaqueta, C.; Luijten, E. *Phys. Rev. Lett.* **2007**, *99*, 138302-1–138302-4.

(42) Grønbech-Jensen, N.; Mashl, R.J.; Bruinsma, R.F.; Gelbart, W.M. *Phys. Rev. Lett.* **1997**, *78*, 2477–2480.

(43) Schmidt, B.; Wandrey, C.; Freitag, R. *J. Chromatogr. A* **2002**, *944*, 149–159.

(44) Mertz, D.; Hemmerlé, J.; Mutterer, J.; Ollivier, S.; Voegel, J.C.; Schaaf, P.; Lavalle, P. *Nano Lett.* **2007**, *7*, 657–662.

(45) Higo, M.; Lu, X.; Mazur, U.; Hipps, K. *Chem. Lett.* **1999**, *28*, 679–680.

(46) Stejskal, E.O.; Tanner, J.E. *J. Chem. Phys.* **1965,** *42*, 288–292; Teller, D.C.; Swanson, E.; de Haen, C. *Methods Enzymol.* **1979,** *61*, 103–124; Cohen, Y.; Avram, L.; Frish, L. *Angew. Chem., Int. Ed.* **2005,** *44*, 520–554.